Medium effects in the production and decay of ω- and ρ-resonances in pion-nucleus interactions*

W. Cassing[1], Ye.S. Golubeva[2], A.S. Iljinov[2]
and L.A. Kondratyuk[3]

[1] Institute for Theoretical Physics, University of Giessen, D-35392 Giessen, Germany
[2] Institute of Nuclear Research, 117312 Moscow, Russia
[3] Institute of Theoretical and Experimental Physics, 117259 Moscow, Russia

Abstract

The ω- and ρ-resonance production and their dileptonic decay in $\pi^- A$ reactions at GSI energies are calculated within the intranuclear cascade (INC) approach. The invariant mass distribution of the dilepton pair for each resonance is found to have two components which correspond to the decay of the resonances outside and inside the target nucleus. The latter components are strongly distorted by the nuclear medium due to resonance-nucleon scattering and a possible mass shift at finite baryon density. These medium modifications are compared to background sources in the dilepton spectrum from πN bremsstrahlung and the Dalitz decays of Δ's, ω and η mesons produced in the reaction.

*Supported by DFG

The question about the properties of hadronic resonances in the nuclear medium has received a vivid attention during the last years (cf. Refs. [1, 2, 3, 4]). Here, QCD inspired effective Lagrangian models [1, 2] or approaches based on QCD sum rules [3, 4] predict that the masses of the vector mesons ρ, ω and ϕ should decrease with the nuclear density. Furthermore, along with a dropping mass the phase space for the resonance decay also decreases which results in a modification of the resonance width in matter. On the other hand, due to collisional broadening - which depends on the nuclear density and the resonance-nucleon interaction cross section (cf. Refs. [5, 6]) - the resonance width should increase again.

The in-medium properties of vector mesons have been addressed experimentally so far by dilepton measurements at the SPS, both for proton-nucleus and nucleus-nucleus collisions [7, 8, 9]. As proposed by Li *et al.* [10], the enhancement in $S + Au$ reactions compared to $p + Au$ collisions in the invariant mass range $0.3 \leq M \leq 0.7$ GeV might be due to a shift of the ρ meson mass. The microscopic transport studies in Refs. [11, 12] for these systems point in the same direction, however, also more conventional selfenergy effects cannot be ruled out at the present stage [11, 13]. It is therefore necessary to have independent information on the vector meson proporties from reactions, where the dynamical picture is more transparent, i.e. in pion-nucleus collisions. Here, especially the ω meson can be produced with low momenta in the laboratory system, such that a substantial fraction of them will still decay inside a heavy nucleus [14].

The mass distributions of the vector mesons in the latter case are expected to have a two component structure [6] in the dilepton invariant mass spectrum: the first component corresponds to resonances decaying in the vacuum, thus showing the free spectral function which is very narrow in case of the ω meson; the second (broad) component then corresponds to the resonance decay inside the nucleus. We will use that (in first order) the in-medium resonance can also be described by a Breit- Wigner formula with a mass and width distorted by the nuclear environment.

In this letter we present first microscopic calculations for the production and dileptonic decay of ω and ρ resonances in $\pi^- A$ collisions at pion momenta of 1.3 GeV/c available at GSI in the near future. The calculations are performed within the framework of the intranuclear cascade model (INC) [15] which was extended earlier [16, 17] to account for the in-medium resonance decays. First calculations for the shapes of the ω and ρ peaks in proton (antiproton) induced reactions $pA \to VX \to e^+e^-X$

($\bar{p}A \to VX \to e^+e^-X$) have been reported in Refs. [16, 17]. Here we consider explicitly π^- induced reactions and also compute the background sources in the dilepton spectrum from nucleon-nucleon and pion-nucleon bremsstrahlung as well as the Dalitz decays $\Delta \to Ne^+e^-$, $\omega \to \pi^0 e^+e^-$ and $\eta \to \gamma e^+e^-$ following Refs. [11, 12, 18].

The vector mesons ρ, ω are produced in the first hard pion-nucleon collision in the target and propagate through the rest of the nucleus. If the wave length of the produced meson is much smaller than the nuclear radius, it is possible to use the eikonal approximation for the Green function describing its propagation from the point $\vec{r} = (\vec{b}, z)$ to $\vec{r}' = (\vec{b}', z')$ [6],

$$G_k(\vec{b}', z'; \vec{b}, z) = \frac{1}{2ik} exp\{i \int_z^{z'} [k + \frac{1}{2k}(\Delta + 4\pi f(0)\rho(\vec{b}, \zeta)] d\zeta\} \times \delta(\vec{b} - \vec{b}')\theta(z' - z), \tag{1}$$

where the z-axis is directed along the resonance momentum $\vec{k}$, $\vec{b}$ is the impact parameter, $f(0)$ is the resonance–nucleon forward scattering amplitude, ρ is the nuclear density and Δ is the inverse resonance propagator

$$\Delta = P^2 - M_R^2 + iM_R\Gamma_R \tag{2}$$

with M_R, Γ_R and P being the mass, width and four momentum of the resonance. The latter can be defined through the four momenta of its decay products

$$P = p_1 + p_2 + ... \tag{3}$$

Let us now consider the production of the vector mesons ρ and ω in the nuclear target and their decay into the e^+e^- pair:

$$\pi^- A \to RX \to e^+e^-X. \tag{4}$$

If the resonance R is created at $(\vec{b}, z)$ and decays in $(\vec{b}', z')$, the exponent of the Green function (1) can be separated into the contributions from the two regions

1) $z \le z' \le z_s = \sqrt{R^2 - \vec{b}^2}$ and
2) $z' \ge z_s = \sqrt{R^2 - \vec{b}^2}$.

When the resonance decays inside the nucleus of radius R, only the first part contributes and the inverse resonance propagator has the form

$$\Delta^* = \Delta + 4\pi f(0)\rho_0 = P^2 - M_R^{*2} + iM_R^*\Gamma_R^* \tag{5}$$

where

$$M_R^{*2} = M_R^2 - 4\pi Ref(0)\rho_0, \tag{6}$$

$$M_R^*\Gamma_R^* = M_R\Gamma_R + 4\pi Imf(0)\rho_0. \tag{7}$$

If the resonance decays outside the nucleus, both regions contribute and the probability for lepton pair production with total momentum $\vec{P}$ and invariant mass squared P^2 can be written as

$$|M(\vec{P},P^2)|^2 = N|f_{\pi^- N\to RX}|^2 \int d^2\vec{b}dz\ \rho(\vec{b},z)|A_{in}(\vec{P},P^2;\vec{b},z) + A_{out}(\vec{P},P^2;\vec{b},z)|^2. \tag{8}$$

In Eq. (8) the contributions from the first and second part can be written as

$$A_{in}(\vec{P},P^2;\vec{b},z) = \frac{1 - exp[i(\Delta^*/2k)(z_s - z)]}{\Delta^*}, \tag{9}$$

and

$$A_{out} = \frac{exp[i(\Delta^*/2k)(z_s - z)]}{\Delta}, \tag{10}$$

where $f_{\pi^- N\to RX}$ is the amplitude for the resonance production on a nucleon in the channel RX and N is the normalization factor which contains the branching ratio $R \to e^+e^-$.

When the resonance decays inside the nucleus, its form is described by the Breit–Wigner formula (9) with Δ^* from (5), that contains the effects of collisional broadening

$$\Gamma_R^* = \Gamma_R + \delta\Gamma, \tag{11}$$

where

$$\delta\Gamma = \gamma v \sigma_{(RN)}\rho_B, \tag{12}$$

and a shift of the meson mass

$$M_R^* = M_R + \delta M_R, \tag{13}$$

where

$$\delta M_R = -\gamma v \sigma_{(RN)}\rho_B \alpha. \tag{14}$$

In Eqs. (12) and (14) v is the resonance velocity with respect to the target at rest, γ is the associated Lorentz factor, ρ_B is the nuclear density, $\sigma_{(RN)}$ is the resonance–nucleon total cross section and $\alpha = (Ref(0))/(Imf(0))$.

If the ratio α is small - which is actually the case for the reactions considered because many reaction channels are open - the broadening of the resonance will be the main

effect. The sign of the mass shift depends on the sign of the real part of the forward RN scattering amplitude which, in principle, also depends on the momentum of the resonance. For example, at low energy various authors [1, 2, 3, 4] predict a decreasing mass of the vector mesons ρ, ω and ϕ with the nucleon density, whereas Eletsky and Ioffe have argued recently [19] that the ρ might become heavier in nuclear matter at energies of 2-7 GeV.

In the following we consider the reaction $\pi^- A \to VX \to e^+e^-X$ for Pb-targets at a pion momentum of 1.3 GeV/c. The yields of ω – and ρ– mesons are calculated within the framework of the intranuclear cascade model developed in Ref. [15], where the nucleus is devided into series of concentric zones and it is possible to follow the propagation of each produced particle from one zone to another. The decay of the resonances to e^+e^- with their actual spectral shape was performed here as in Refs. [16, 17]. The calculation proceeds as follows: when the resonance decays into dileptons inside the nucleus its mass is generated according to the Breit–Wigner distribution with $M_R^* = M_R + \delta M_R$ and $\Gamma_R^* = \Gamma_R + \delta\Gamma_R$, where the collisional broadening and the mass shift are calculated according to the local nuclear density. Its decay to dileptons is recorded as a function of the corresponding invariant mass bin and the local density. If the resonance leaves the nucleus, its spectral function automatically coincides with the free distribution because δM_R and $\delta\Gamma_R$ are zero in this case (cf. Eqs. (12), (14)).

For the ω production we consider the channels: $\pi^- p \to \omega n$ and $\pi^- n \to \omega\pi^- n$ with parametrizations from Ref. [20]. Though the momentum of 1.3 GeV/c is smaller than the threshold momentum for the second channel, it contributes to ω production in $\pi^- A$ collisions due to the Fermi motion of the target nucleons. For ρ-meson production we use the same cross sections as for ω-mesons; this holds experimentally within 20%.

The resulting momentum distribution of all decaying ω-mesons and those decaying inside the nucleus (at densities $\rho \geq 0.03\rho_0$) are displayed in Fig. 1 by the solid and dotted histograms, respectively. They extend to 1.1 GeV/c with average momenta of about 0.65 and 0.53 GeV/c, respectively. The bump in the full spectrum around 0.5 GeV/c describes the contribution of the channel $\pi^- n \to \omega\pi^- n$. Using a cut of $0.03\rho_0$, approximately 47% of the produced ω- mesons are absorbed at finite density. We note that the ω-mesons decaying outside the nucleus show a momentum distribution very similar to the solid curve in Fig. 1 especially at high laboratory momenta. On the other hand, ω mesons with low momenta to a large extend still decay within the target nucleus.

In Fig. 2a we present the e^+e^- mass spectrum from ω- decays neglecting collisional broadening, however, including a medium dependent ω-mass as suggested by Hatsuda and Lee [3]

$$M_R^* = M_R(1 - 0.18\rho_B(r)/\rho_0), \tag{15}$$

where $\rho_B(r)$ is the nuclear density at the resonance decay and $\rho_0 = 0.16 fm^{-3}$. Fig. 2a describes the full mass distribution whereas Fig. 2b includes a cut in the ω momentum for $p_{lab} \leq 0.4 GeV/c$. The shaded histograms describe the contributions of the '*in*' components, while the solid histograms are the sum of the '*in*' and '*out*' components. Due to sizeable surface effects (with lower nucleon density) the mass distribution of the '*in*' components is spread out. Nevertheless, we still observe two sharp peaks corresponding to the in-medium and vacuum masses, respectively. As expected from Fig. 1, a cut in the momentum distribution for $p_{lab} \leq 0.4$ GeV/c enhances the contribution from the '*in*' component relative to the '*out*' component (Fig. 2b).

In Fig. 2c we show the dilepton spectrum from ω decays when a mass shift and collisional broadening are taken into account. Here we have parametrized the momentum dependent $\omega - N$ cross section by

$$\sigma_{\omega N}(p_{lab}) = A + B/p_{lab} \tag{16}$$

with $A = 11 mb$ and $B = 9 mb * GeV/c$, which is taken as a guide due to the lack of experimental data[1]. Furthermore, we have assumed $\sigma_{\rho N} \approx \sigma_{\pi N}$ in our calculations for $\rho + N$ collisions. Again the relative contribution of the '*in*' component (shaded histograms) in the e^+e^- invariant mass spectrum considerably increases when ω-mesons with momenta less than 0.4 GeV/c are selected (Fig. 2d). Due to collisional broadening the width of the '*in*' component increases substantially relative to the free ω width such that a pronounced peak for the '*in*' component can no longer be observed.

Whereas the ω dilepton mass distributions show quite considerable changes for the different scenarios proposed, it is questionable if these modifications actually can be seen when including all other known sources of dilepton channels, i.e. π-nucleon and proton-neutron bremsstrahlung, the Dalitz decays of the η, ω and Δ as well as the direct decay of the ρ^0 meson. The individual branching ratios and formfactors for the latter processes are taken from Ref. [11, 12], while the bremsstrahlung channels are evaluated in the soft photon approximation [18], which will provide an upper estimate for the dilepton yield from bremsstrahlung.

[1] The respective cross section in ref. [21] is too large by about a factor of 2.

In Fig. 3 we show the inclusive dilepton spectrum for $\pi^- + \mathrm{Pb}$ at 1.3 GeV/c - in logarithmic representation - from the various channels described above including collisional broadening, however, no mass shifts of the ω and ρ mesons in the medium. The dominant background processes are seen to result from pion-nucleon (πN) bremsstrahlung, the η Dalitz decay (denoted by η; solid line) and the ω Dalitz decay ($\omega \to \pi^0 e^+ e^-$). The Δ Dalitz decay (Δ) as well as proton-neutron (pn) bremsstrahlung are of minor importance. The upper solid curve represents the sum of all contributions. We note that the width of the ρ–peak here is about 220 MeV, which is essentially larger than its vacuum width $\Gamma_\rho \approx 150$ MeV due to collisional broadening as described above. Nevertheless, above about 0.65 GeV of invariant mass M the spectrum is fully dominated by the vector meson decays with a low background.

In Fig. 4 we show the resulting inclusive dilepton spectrum for the same system including collisional broadening as well as mass shifts of the ω and ρ mesons in the medium according to Eq. (15). The background processes here are practically the same as in Fig. 3 and dominate for $M \leq 0.6$ GeV. When comparing the total spectrum from Fig. 3 with that from Fig. 4 we find an enhancement by a factor of 2 for $0.65 \leq M \leq 0.75$ GeV for the dropping vector meson masses as well a decrease of the spectrum for $M \geq 0.85$ GeV due to the shifted ρ mass because the ρ almost completely decays inside the Pb-nucleus. The relative modifications of the dilepton spectra are qualitatively very similar to the situation at SPS energies in case of nucleus-nucleus collisions [22], when employing a mass resolution of $\Delta M = 10$ MeV as in the present case. Thus dileptons from pion-nucleus reactions at much lower energy also qualify for the experimental investigation of in-medium vector meson properties.

In summary, we have presented first calculations for dilepton production in pion-nucleus reactions and investigated the various contributing channels as well as in-medium modifications of the vector mesons due to collisional broadening or in-medium mass shifts [1, 2, 3, 4]. Our results for π^-+ Pb at 1.3 GeV/c indicate that the dominant background for invariant masses M above 0.6 GeV arises from $\pi^- N$ bremsstrahlung which, however, is still small compared to the yield from the direct vector meson decays. A mass shift of the ρ and ω mesons should be seen experimentally by an enhanced yield in the mass regime $0.65 \leq M \leq 0.75$ GeV and a mass shift of the ρ meson especially for $M \geq 0.85$ GeV because the ρ almost completely decays inside a Pb-nucleus. The in-medium modifications of the ω mesons are most pronounced for small momentum cuts on the e^+e^- pair in the laboratory. This, however, will require a high mass resolution

at least in the order of the free ω width.

The authors acknowledge many helpful discussions with E.L. Bratkovskaya and A. Sibirtsev throughout this study.

References

[1] G. Brown and M. Rho, Phys. Rev. Lett. 66 (1991) 2720.

[2] C.M. Shakin and W.-D. Sun, Phys. Rev. C 49 (1994) 1185.

[3] T. Hatsuda and S. Lee, Phys. Rev. C 46 (1992) R34.

[4] M. Asakawa and C.M. Ko, Phys. Rev. C 48 (1993) R526.

[5] L. A. Kondratyuk, M. Krivoruchenko, N. Bianchi, E. De Sanctis and V. Muccifora, Nucl. Phys. A 579 (1994) 453.

[6] K.G. Boreskov, J. Koch, L.A. Kondratyuk and M.I. Krivoruchenko, Proc. of the 3rd International Conference on Nucleon-Antinucleon Physics (NAN'95), Phys. of Atomic Nuclei 10 (1996) 1908.

[7] G. Agakichiev et al., Phys. Rev. Lett. 75 (1995) 1272.

[8] M.A. Mazzoni, Nucl. Phys. A 566 (1994) 95c.

[9] T. Akesson et al., Z. Phys. C 68 (1995) 47.

[10] G.Q. Li, C.M. Ko, and G.E. Brown, Phys. Rev. Lett. 75 (1995) 4007.

[11] W. Cassing, W. Ehehalt and C.M. Ko, Phys. Lett B 363 (1995) 35.

[12] W. Cassing, W. Ehehalt and I. Kralik, Phys. Lett B 377 (1996) 5.

[13] R. Rapp, G. Chanfray, and J. Wambach, Phys. Rev. Lett. 76 (1996) 368.

[14] V. Metag, private communication.

[15] Ye.S. Golubeva, A.S. Iljinov, B.V. Krippa and I.A. Pshenichnov, Nucl. Phys. A 537 (1992) 393.

[16] Ye.S. Golubeva, A.S. Iljinov and L.A. Kondratyuk, Proc. of the 3rd International Conference on Nucleon-Antinucleon Physics (NAN'95), Phys. of Atomic Nuclei No.10 (1996) 1894.

[17] Ye.S. Golubeva, A.S. Iljinov and L.A. Kondratyuk, Proc. of the 3rd International Conference "Mesons-96", Cracow, May 1996, to be published by World Scientific, Singapore, 1997.

[18] Gy. Wolf, G. Batko, W. Cassing et al., Nucl. Phys. A 517 (1990) 615;
Gy. Wolf, W. Cassing and U. Mosel, Nucl. Phys. A 552 (1993) 549.

[19] V. Eletsky and B.L. Ioffe, Preprint KFA-IKP(TH)-1996-10.

[20] A. Sibirtsev, Nucl. Phys. A604 (1996) 455;
A. Sibirtsev, W. Cassing and U. Mosel, nucl-th/9607047, Z. Phys. A, in print

[21] Ye.S. Golubeva, A.S. Iljinov and I.A. Pshenichnov, Nucl. Phys. A 562 (1993) 389

[22] E. L. Bratkovskaya and W. Cassing, nucl-th/9611042, submitted to Nucl. Phys. A.

Figure captions

Fig. 1: The momentum distribution of the ω mesons produced in the reaction $\pi^- Pb \to \omega X$ at 1.3 GeV/c in the laboratory; solid histogram: all ω mesons; dotted histogram: those decaying inside the nucleus.

Fig. 2: The e^+e^- mass spectrum from ω-decay when including a medium dependent ω-mass shift according to Hatsuda and Lee ([3]): *a*) and *b*) - without collisional broadening; *c*) and *d*) - with collisional broadening. Figs. *a*) and *c*) describe the full mass distributions, *b*) and *d*) events with a ω momentum cut $p_{lab} \leq 0.4 GeV/c$. The hatched histograms describe the contribution of the '*in*' component, while the solid histograms display the total contribution from the '*in*' and '*out*' components, respectively.

Fig. 3: The dilepton spectra for π^- + Pb reactions at 1.3 GeV/c in logarithmic representation when a mass shift of the vector mesons is neglected and collisional broadening according to Eq. (12) is taken into account. The upper solid curve is the sum of all contributions; the individual channels correspond to the η Dalitz decay (η), pion-nucleon bremsstrahlung (πN), the ω Dalitz decay ($\omega \to \pi^0 e^+ e^-$), the Δ Dalitz decay (Δ), proton-neutron bremsstrahlung (pn), and the direct decays of the vector mesons ρ and ω. The mass resolution adopted is ΔM = 10 MeV.

Fig. 4: The dilepton spectra for π^- + Pb reactions at 1.3 GeV/c in logarithmic representation when including a mass shift of the vector mesons according to Eq. (15) and collisional broadening according to Eq. (12). The notations are the same as in Fig. 3.

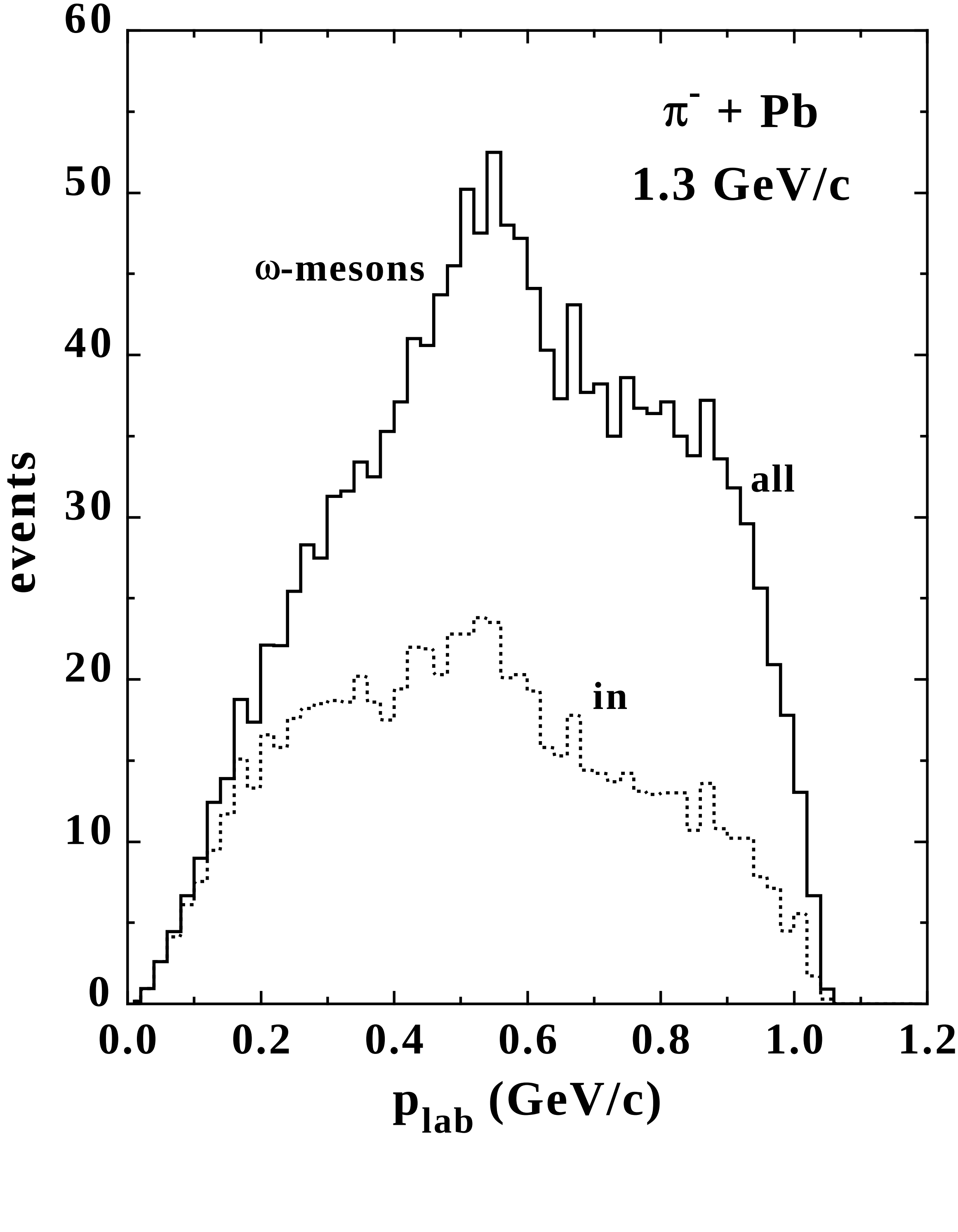

60
50
40
30
20
10
0
events
π⁻ + Pb
1.3 GeV/c
ω-mesons
all
in
0.0
0.2
0.4
0.6
0.8
1.0
1.2
p_lab (GeV/c)

Fig. 1

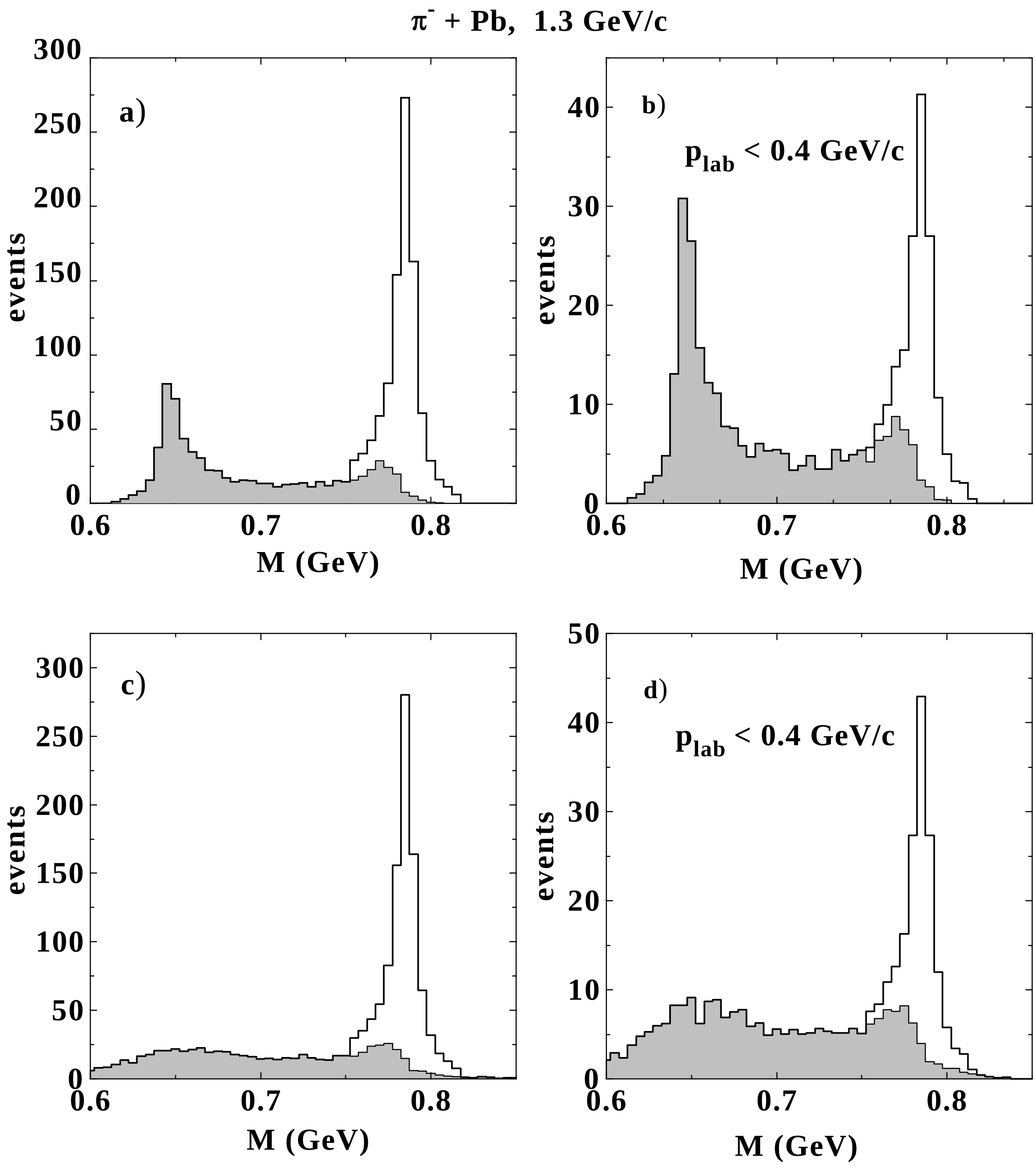

Fig. 2

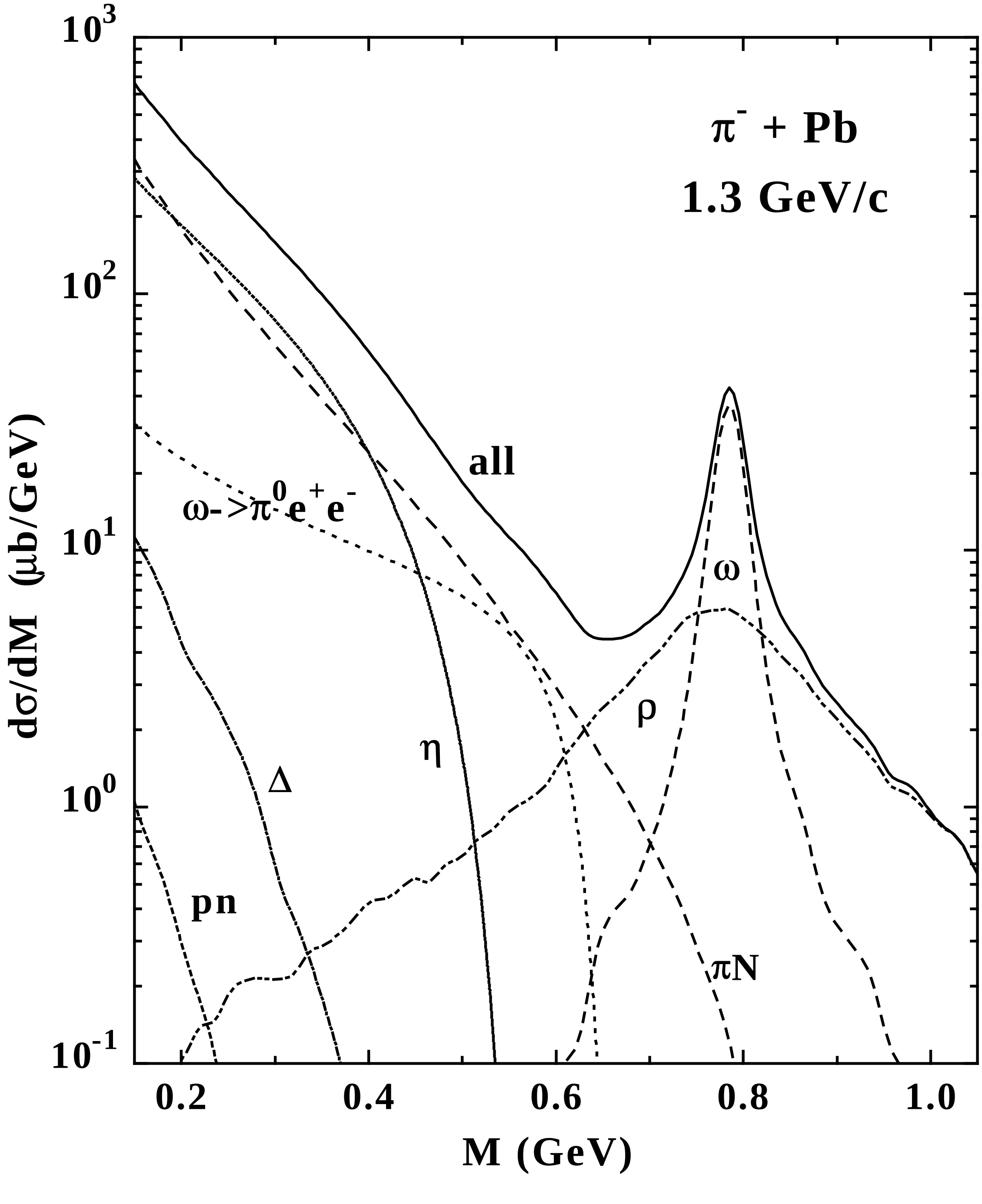

π⁻ + Pb
1.3 GeV/c
all
ω->π⁰e⁺e⁻
ω
ρ
η
Δ
pn
πN
dσ/dM (μb/GeV)
M (GeV)
10³
10²
10¹
10⁰
10⁻¹
0.2
0.4
0.6
0.8
1.0

Fig. 3

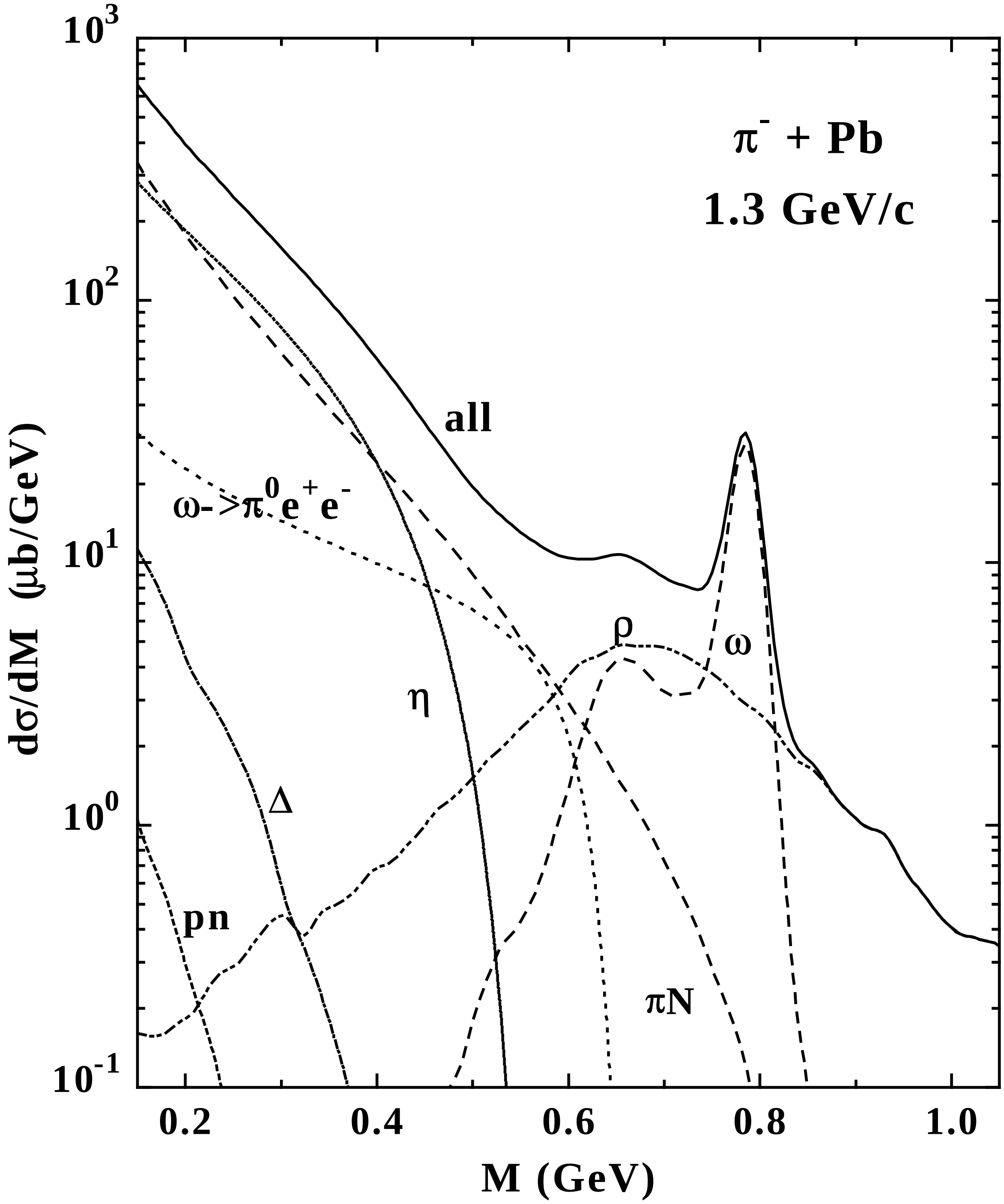

$\pi^- + Pb$
1.3 GeV/c
all
$\omega\text{->}\pi^0 e^+ e^-$
ρ
ω
η
Δ
pn
πN
$d\sigma/dM$ (μb/GeV)
M (GeV)
10^3
10^2
10^1
10^0
10^{-1}
0.2
0.4
0.6
0.8
1.0

Fig. 4